



Ceriotti, Matteo and McInnes, Colin (2014) Design of ballistic three-body trajectories for continuous polar Earth observation in the Earth-Moon system. Acta Astronautica, 102. pp. 178-189. ISSN 0094-5765 , <http://dx.doi.org/10.1016/j.actaastro.2014.06.001>

This version is available at <https://strathprints.strath.ac.uk/48613/>

Strathprints is designed to allow users to access the research output of the University of Strathclyde. Unless otherwise explicitly stated on the manuscript, Copyright © and Moral Rights for the papers on this site are retained by the individual authors and/or other copyright owners. Please check the manuscript for details of any other licences that may have been applied. You may not engage in further distribution of the material for any profitmaking activities or any commercial gain. You may freely distribute both the url (<https://strathprints.strath.ac.uk/>) and the content of this paper for research or private study, educational, or not-for-profit purposes without prior permission or charge.

Any correspondence concerning this service should be sent to the Strathprints administrator: strathprints@strath.ac.uk

TITLE

Design of ballistic three-body trajectories for continuous polar Earth observation in the Earth-Moon system

AUTHOR NAMES AND AFFILIATIONS

Matteo Ceriotti

School of Engineering

University of Glasgow

G12 8QQ

Glasgow, United Kingdom

matteo.ceriotti@glasgow.ac.uk

Phone: +44 (0)141 330 6465

(Corresponding author)

Colin R. McInnes

Advanced Space Concepts Laboratory, Department of Mechanical & Aerospace Engineering

University of Strathclyde

75 Montrose Street, James Weir Building

G1 1XJ

Glasgow, United Kingdom

colin.mcinnnes@strath.ac.uk

Phone: +44 (0)141 548 2049

ABSTRACT

This paper investigates orbits and transfer trajectories for continuous polar Earth observation in the Earth-Moon system. The motivation behind this work is to complement the services offered by polar-orbiting spacecraft, which offer high resolution imaging but poor temporal resolution, due to the fact that they can only capture one narrow swath at each polar passage. Conversely, a platform for high-temporal resolution imaging can enable a number of applications, from accurate polar weather forecasting to Aurora study, as well as direct-link telecommunications with high-latitude regions. Such a platform would complement polar orbiters. In this work, we make use of resonant gravity swing-by manoeuvres at the Moon in order to design trajectories that are suitable for quasi-continuous polar observation. In particular, it is shown that the Moon can flip the line of apsides of a highly eccentric, highly inclined orbit from north to south, without the need for thrust. In this way, a spacecraft can alternatively loiter for an extended period of time above the two poles. In addition, at the lunar encounter it is possible to change the period of time spent on each pole. In addition, we also show that the lunar swing-by can be exploited for transfer to a so-called pole-sitter orbit, i.e. a spacecraft that constantly hovers above one of the Earth's poles using continuous thrust. It is shown that, by using the Moon's gravity to change the inclination of the transfer trajectory, the total Δv is less than using a trajectory solely relying on high-thrust or low-thrust, therefore enabling the launchers to inject more mass into the target pole-sitter position.

Keywords: Continuous polar coverage, Earth-Moon system, Gravity assist, Pole-sitter transfer design, Trajectory design

1. INTRODUCTION

It is widely known that the polar regions of the Earth cannot be monitored from space in the same way as the low-latitude and equatorial regions. Due to the Earth's spin around its polar axis, the equatorial plane offers a useful vantage-point: a spacecraft in geostationary orbit (GEO) is stationary with respect to an observer on the surface of the Earth, thus providing a means for data relay and hemispheric imaging in one single frame.

However, the coverage of GEO spacecraft degrades at higher latitudes, because the spacecraft's elevation angle becomes very low. Therefore, other platforms are currently being used for polar coverage: they include highly eccentric orbits (like Molniya [1]), which use the oblateness of the Earth to maintain the argument of the pericentre constant in time [2]. Their inclination is fixed at a value of 63.4° , which is still relatively low to obtain a satisfactory coverage of the high-latitude regions [3]. Low- and medium-altitude polar orbits (such as Sun-synchronous orbits) are also widely used for polar imaging, due to the high spatial resolution that they can provide; however only a narrow swath is imaged at each polar passage, relying on multiple passages for complete coverage. This results in poor temporal resolution for the entire polar region, as different areas are imaged at different times, hence missing the opportunity to have a simultaneous and continuous real-time view of the pole. In other words, spatial resolution is traded off for temporal resolution.

In this paper, instead, we are interested in studying a platform that offers high temporal resolution, offering a service that is complementing low and medium Earth orbit spacecraft. The reason for this interest originates in a number of potential applications that could be enabled by a platform that can continuously cover the poles. Although high-bandwidth telecommunications and high-resolution imagery are difficult due to the large Earth-spacecraft distance, a number of novel potential applications are enabled, both in the fields of observation and telecommunications. It was shown that spatial resolution in the visible wavelength in the range 10-40 km should be sufficient for real-time, continuous views of dynamic phenomena and large-scale polar weather systems [4]. The creation of atmospheric motion vectors (AMV) would also make use of the stationary location of the platform, avoiding gap problems related to geo-location and inter-calibration that composite images introduce [5]. Glaciology and ice-pack monitoring would also benefit from continuous, but low resolution polar observation [5]. Ultraviolet imagery of the polar night regions at 100 km resolution or better would enable real-time monitoring of rapidly-changing hot spots in the aurora that can affect high frequency communications and radar [4]. The platform could also be used as a continuous data-relay for key Antarctic research activities, in particular for scientific experiments, links to automated weather stations, emergency airfields and telemedicine. Ship tracking was also proposed, to support future high-latitude oil and gas exploration [3].

It is clear that the only platform that can offer the same coverage conditions for the poles as a GEO spacecraft would be a stationary spacecraft aligned with the polar axis. This is known in the literature as a "pole-sitter" or "pole-squatter", and has been investigated since 1980, starting from Driver's analysis [6] up to an end-to-end to end, optimised mission and systems design performed by the authors [7]. The main disadvantages of this type of spacecraft is the considerable distance from the Earth, as well as the need for continuous low-thrust in order to

maintain its vantage position, and therefore the mission lifetime is seriously affected by the availability of propellant mass on-board.

To overcome these limits, other concepts were investigated the literature, including the use of solar sailing [8, 9]. Recently, work performed by the authors investigated alternative mission scenarios in the Sun-Earth system, including optimised pole-sitters and periodic high-amplitude vertical Lyapunov orbits [10].

The aim of this paper is to explore possible mission scenarios for continuous polar coverage using periodic trajectories in the Earth-Moon system. Past studies in the literature showed the possibility of using a gravity assist at the Moon to change the orbital plane of a spacecraft with respect to the lunar orbital plane [11], without the need of expensive thrusting manoeuvres. This idea can be exploited for reaching orbits that pass over the Earth's poles at little cost, or indeed used for the transfer to the pole-sitter position. The so-called lunar backflip orbits were also studied in the literature [12, 13], however while one leg of the orbit hovers over a pole of the Earth, the second one has a very low inclination, therefore not offering any possibility of polar coverage. In this work, we use a patched-conic approximation to design Earth-centred orbits that exploit the swing-by of the Moon to achieve the desired orbital elements.

The paper is organised as follows. Initially, the dynamics of the lunar swing-by is explained in Section 2, together with the two methods that will be used, throughout the work, to solve the resulting velocity triangles. Section 3 then describes the orbits for polar observation, including a strategy to flip the line of the nodes and therefore observe the North Pole and the South Pole alternatively, and also change the period of observation of each pole. Section 4 investigates the use of the lunar swing-by to design a transfer to the pole-sitter position, and it includes a preliminary assessment of the mass that can be injected into the poles-sitter position using Ariane 5 and Soyuz.

2. LUNAR SWING-BY

This section shows the methodology followed to solve the ballistic swing-by at the Moon [14]. We approximate the Moon's orbit as a perfectly circular orbit around the Earth, at radius $r_M = 384,401$ km, with velocity $v_M = \sqrt{\mu/r_M}$, with $\mu = 3.9860 \times 10^5$ km³s⁻² the planetary gravitational parameter of the Earth.

Let us call \mathbf{v} the absolute velocity vector at the Moon, and denote with a superscript “-” the incoming conditions just before the swing-by manoeuvre, and with “+” the outgoing ones, just after the manoeuvre.

One assumption that is being made, and that will be used throughout the paper, is that in the outgoing orbit, the anomaly of the pericentre is $\omega = \pi/2$ or $\omega = 3\pi/2$ and the swing-by is at a true anomaly $\theta = \pi/2$ or $\theta = 3\pi/2$.

Some of these orbits are represented in Fig. 4, for a specific inclination. This also implies that the line of the nodes of the outgoing orbit coincides with the semi-latus rectum direction, and that the anomaly of the pericentre is either $\pi/2$ or $3\pi/2$. This translates into the following relation between the outgoing velocity v^+ and the flight path angle γ^+ :

$$p = r_M = \frac{h^2}{\mu} = \frac{(r_M v^+ \cos \gamma^+)^2}{\mu} \quad (1)$$

$$\gamma^+ = \pm \arccos \left(\frac{\sqrt{r_M \mu}}{r_M v^+} \right) \quad (2)$$

where p is the semi-latus rectum length.

Note that this relationship introduces a constraint on v^+ such that γ^+ exists; it must be

$$\frac{\sqrt{r_M \mu}}{r_M v^+} \leq 1$$

or

$$v^+ \geq \sqrt{\frac{\mu}{r_M}} = v_M$$

Let us consider a reference frame centred in the Moon, aligned with the radial, transversal and out-of-plane directions of the Moon's orbit. In this frame, the velocity of the Moon, purely transversal, is:

$$\mathbf{v}_M = [0, v_M, 0]^T$$

where $v_M = \sqrt{\mu/r_M}$

The incoming relative velocity, at infinity of the swing-by hyperbola, is:

$$\mathbf{v}_\infty^- = \mathbf{v}^- - \mathbf{v}_M \quad (3)$$

As well known in the literature, a ballistic swing-by does not change the magnitude of the velocity at infinity, but only its direction. Therefore it is possible to define a $v_\infty = \text{constant}$ sphere around \mathbf{v}_M , which represents all hyperbolas with the same energy around the Moon. The outgoing absolute velocity vector shall stay on this spherical surface (represented in grey in Fig. 1 and Fig. 2). However, the exact position on the surface is yet to be determined. Two procedures will be used, depending on whether the outgoing orbit inclination is given, or the semi-major axis.

2.1. Outgoing inclination given

In this case, the inclination of the outgoing orbit is known, therefore the outgoing velocity vector must lie on a plane that is inclined at i^+ around the radial direction, measured from the Moon's orbit plane. This plane is in red in Fig. 1.

When an intersection exists, this is a circumference, whose radius is $\overline{CD} = \sqrt{v_\infty^2 - (v_M \sin i^+)^2}$, and \mathbf{v}^+ is on this

circumference (see Fig. 1 for defining points and segments). Instead, if the plane does not intersect the sphere (i.e. $v_\infty < v_M \sin i^+$), then no solution is possible, i.e. either the incoming velocity vector or the outgoing inclination shall be changed.

In order to define the position of \mathbf{v}^+ on the circumference, we introduce a parameterisation through an angle α , that is the angle between the radius defining the vector \mathbf{v}^+ and a radius aligned on the radial direction. With this choice, we have the following outgoing velocity and flight path angle:

$$v^{+2}(\alpha) = \overline{CD}^2 + \overline{AC}^2 - 2\overline{CD} \overline{AC} \cos\left(\frac{\pi}{2} + \alpha\right) \quad (4)$$

$$\gamma^+(\alpha) = \arccos\left(\frac{v^{+2} + \overline{AC}^2 - \overline{CD}^2}{2v^+ \overline{AC}}\right) \quad (5)$$

However, the flight path angle can also be expressed through Eq. (2). The value of α can then be found numerically, through a line search, by equating Eq. (2) to Eq. (5). Once α is known, Eq. (4) and (5) can be used to determine γ^+ and v^+ .

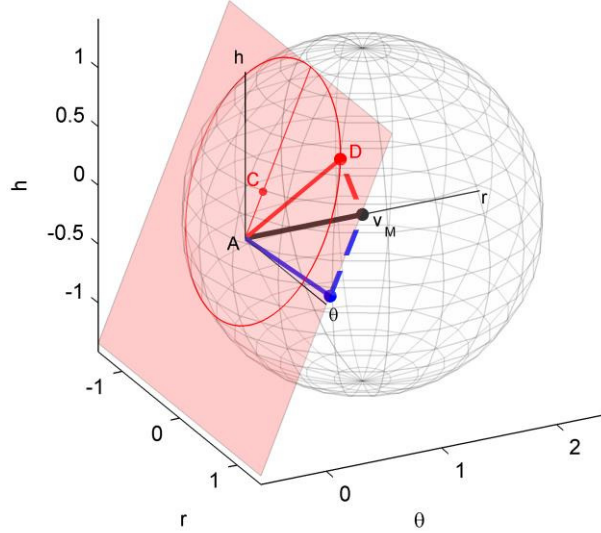


Fig. 1. Velocity vectors of the swing-by with outgoing inclination given. Only solution with γ^+ is represented. Bold segments are velocity vectors. Dashed segments are velocities relative to the Moon. Blue refers to incoming vectors, red refers to outgoing vectors. Black vectors refer to the Moon orbit.

2.2. Outgoing semi-major axis given

In this second case, we assume that the semi-major axis of the outgoing orbit is given. Note that, since the semi-latus rectum of the orbit is fixed, see Eq. (1), equivalently any other in-plane parameter could be provided.

The outgoing absolute velocity magnitude can immediately be computed through the orbital energy:

$$v^+ = \sqrt{\frac{2\mu}{r_M} - \frac{\mu}{a^+}}$$

Now Eq. (2) can be used to find the flight path angle γ^+ . All possible outgoing orbits will differ in inclination, but have the same γ^+ and v^+ . This means that all possible \mathbf{v}^+ define two conical surfaces around the radial direction (in red in Fig. 2): each cone spans all possible inclinations of outgoing orbit, and the two cones refer to the two cases $\gamma^+ > 0$, $\gamma^+ < 0$. Since the vector \mathbf{v}^+ shall also lie on the sphere, then the problem is to find the intersection between the circumference defining the base of the cone and the sphere. The vector \mathbf{v}^+ can be parameterised as a function of the unknown inclination:

$$\mathbf{v}^+(\mathbf{i}^+) = v^+ \begin{bmatrix} \cos \gamma^+ \\ \sin \gamma^+ \cos i^+ \\ \cos \gamma^+ \sin i^+ \end{bmatrix} \quad (6)$$

This can be used to compute the magnitude of the outgoing relative velocity as:

$$v_\infty(\mathbf{i}^+) = \left| \mathbf{v}^+(\mathbf{i}^+) - \mathbf{v}_M \right| \quad (7)$$

The magnitude of v_∞ can also be expressed through Eq. (3), therefore analogously to the previous case, the value of i^+ can then be found through a line search, by equating Eq. (3) to Eq. (7). Once i^+ is known, Eq. (6) can be used to determine \mathbf{v}^+ .

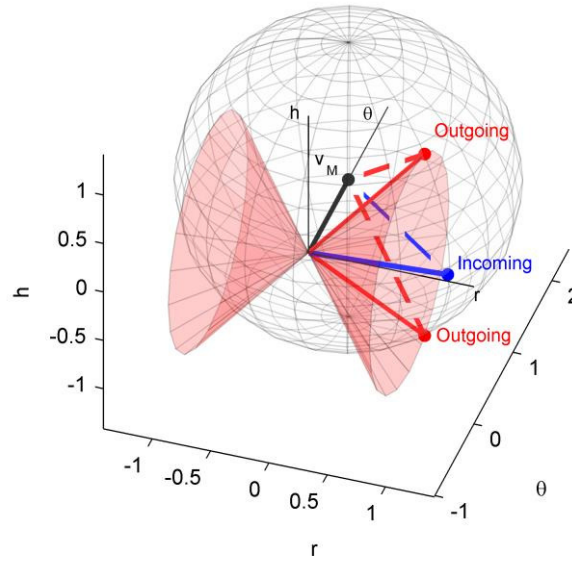


Fig. 2. Velocity vectors of the swing-by with outgoing semi-major axis given. Only solutions with γ^+ are represented. Bold segments are velocity vectors. Dashed segments are velocities relative to the Moon. Blue refers to incoming vectors, red refers to outgoing vectors. Black vectors refer to the Moon orbit.

2.3. Swing-by hyperbola

For both cases presented before, the outgoing relative velocity is computed as:

$$\mathbf{v}_\infty^+ = \mathbf{v}^+ - \mathbf{v}_M$$

and it can be used to compute the pericentre of the swing-by hyperbola, as:

$$\delta_{sb} = \arccos \left(\frac{\mathbf{v}_\infty^- \cdot \mathbf{v}_\infty^+}{v_\infty^2} \right)$$

$$e_{sb} = \left(\sin \frac{\delta_{sb}}{2} \right)^{-1}$$

$$r_{p, sb} = \frac{\mu_M (e_{sb} - 1)}{v_\infty^2}$$

The swing-by is feasible if:

$$r_{p, sb} > R_M \quad (8)$$

where $R_M = 1738 \text{ km}$ is the radius of the Moon, and the gravitational parameter of the Moon is $\mu_M = 4902.8 \text{ kg}^3\text{s}^{-2}$.

3. POLAR OBSERVATION ORBITS

In this section, we will devise a strategy for covering both North and South Poles, involving a sequence of lunar swing-bys to change the orbital parameters.

The lunar orbit is inclined 5.145° to the ecliptic, and due to the precession of the nodes (one revolution every 18.6 years), and the obliquity of the Earth's equator with respect to the ecliptic of 23.44° , the inclination with respect to the Earth's equator varies between 18.29° and 28.58° . For sake of simplicity, in this work it is assumed that this inclination fixed to $i_{eq} = 23^\circ$.

These trajectories are based on the work of Uphoff [15] and Uphoff et al. [11], following a suggestion of Edwin "Buzz" Aldrin. In that work, the concept of a lunar cyclor was described, in which a 180° Moon-to-Moon "backflip" transfer is used to generate a "lunar cyclor" (see Fig. 3, taken from Uphoff et al. [11]): a spacecraft is injected from Earth into an eccentric orbit targeting the Moon; a lunar swing-by modifies the orbital elements to achieve an orbit that is inclined ($\sim 45^\circ$) and encounters the Moon again after half a lunar period; finally, a second lunar swing-by directs the spacecraft into a planar, eccentric orbit passing close to the Earth.

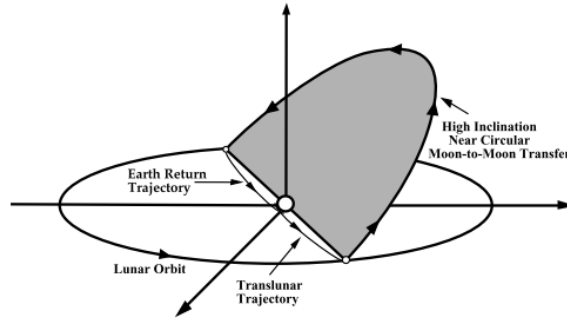


Fig. 3. 180° Moon-to-Moon backflip transfer, as described by Uphoff et al.[11] [Image taken from the same source]

In that work, the inclined orbit of the cyclor is chosen in order to re-encounter the Moon with some relative velocity. However, it is interesting to see that such orbits offer polar coverage for a certain amount of time. This time could be extended by considering orbits with greater semi-major axis, but still such that they re-encounter the Moon at the line of the nodes. Since the orbit of the Moon is almost circular (and assumed exactly circular in this paper), the two encounters shall happen at the two points in which the orbit has the same distance from the focus, i.e. the semi-latus rectum. This also justifies the assumption made in the previous section, where the outgoing orbit anomaly of pericentre had to be $\pi/2$ or $3\pi/2$.

In addition, in order to encounter the Moon with the right timing at the node, it is necessary that the following relationship holds:

$$\bar{P} \equiv t(\theta = \pi/2) - t(\theta = 3\pi/2) = (n + 0.5)P_M$$

\bar{P} represents the time between two lunar encounters, or between the ascending node and the descending node of the orbit, passing from the apocentre. $t(\theta)$ is the time at true anomaly θ , which can be found through the eccentric anomaly and Kepler's equation:

$$E(\theta) = 2 \arctan \left(\sqrt{\frac{1-e}{1+e}} \tan \frac{\theta}{2} \right)$$

$$t = \frac{2\pi}{P_M} (E(\theta) - e \sin E(\theta))$$

$P_M = 27.45$ d is the period of the Moon, and $n \geq 0$ is an integer that defines the number of resonances with the Moon, i.e. the number of full revolutions of the Moon between the two lunar encounters.

Table 1 shows the in-plane Keplerian elements for a number of these orbits.

Table 1. Period between lunar passages and in-plane Keplerian elements for orbits resonant with the Moon.

Period between lunar passages, \bar{P}	Semi-major axis, a , $\times 10^6$ km	Eccentricity, e
$0.5P_M = 13.726$ d	0.3844	0
$1.5P_M = 41.178$ d	0.5657	0.5662
$2.5P_M = 68.630$ d	0.7560	0.7011
$3.5P_M = 96.082$ d	0.9273	0.7652
$4.5P_M = 123.534$ d	1.0847	0.8035

If coverage of the North and South Pole is needed, then the swing-by of the Moon can be used to rotate the line of the nodes by 90° , without changing the inclination of the orbit. This means that if the pericentre of the incoming orbit is on the north side, the outgoing orbit will have its pericentre in the south side. In other words, the pericentre and apocentre directions are inverted, as illustrated in Fig. 4. In particular, the figure plots, for the orbits in Table 1, flipped orbits with the same period.

We note that, in the particular case when the incoming and outgoing orbits have the same in-plane orbital elements and the same inclination, the velocity change required at the lunar swing-by corresponds to a change in sign of the radial component of the velocity.

Flipping the line of apsides is not always possible with a swing-by of the Moon. Depending on the incoming and outgoing velocity vectors, the required deflection might be too high, and therefore the constraint (8) is not satisfied. In order to understand when such a manoeuvre can be done, Fig. 5 shows contours of constant radius of pericentre $r_{p, sb}$ that is required for such manoeuvre at the Moon, depending on the inclination and the semi-major axis (equal for both incoming and outgoing orbits). The vertical dashed lines, plotted for convenience, show the semi-major axis of the orbits with the resonance indicated by the number on the line ($n + 0.5$). The black contour line, corresponding to $r_{p, sb} = 1$ represents the bound of the feasible solutions, and shows that a higher inclination is necessary as the period increases. For example, it is possible to flip the line of apsides of an orbit inclined 40° if $n = 2$, but not if $n = 3$ or more.

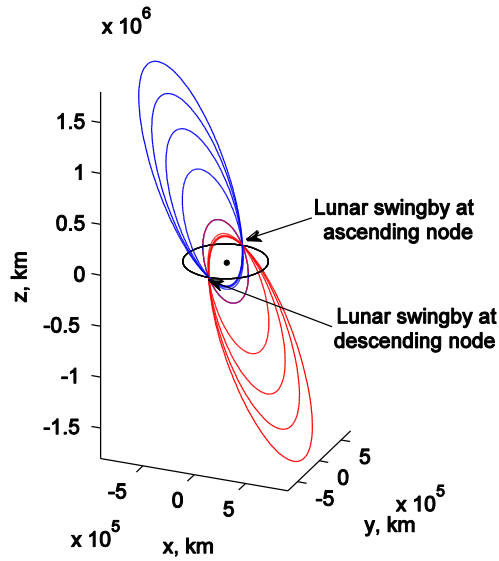


Fig. 4. Effect of rotation of the line of apsides without changing the other orbital elements, for the orbits in Table 1, and arbitrary inclination of 67° .

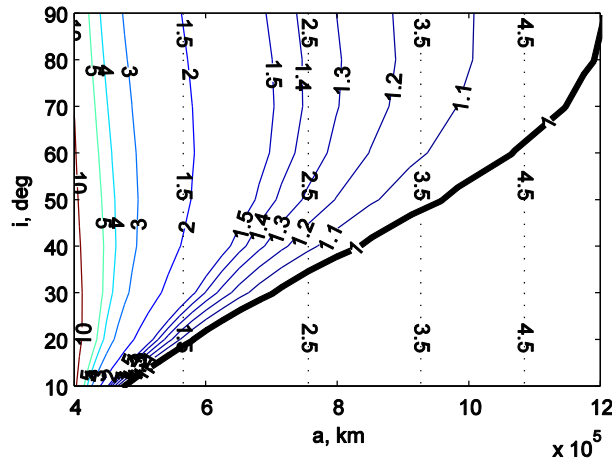


Fig. 5. Pericentre of the swing-by hyperbola (normalised on the lunar radius) necessary to rotate the line of nodes 90° , depending on the semi-major axis and the inclination of the orbit.

Because of the same incoming and outgoing orbital periods, both the orbits will encounter the Moon each time they reach the line of the nodes. However, a more general case exists, in which the outgoing orbit does not have the same period as the incoming one, but just one of the periods listed in Table 1: in this way, there will be again a lunar encounter at each nodal crossing. Assuming that the incoming orbit has an inclination of 67° (i.e. aligned with polar axis), and applying the swing-by solution method in Section 2.2, it is possible to find the data in Table 2. For different periods of the incoming and outgoing orbits, the table shows the inclination of the outgoing orbit. It is worth noting that, for small changes in inclination, that do not affect the coverage of the pole, it is possible to achieve substantial changes of the period of the orbit. For example, for an incoming orbit of $n = 2$, the outgoing orbit can have $n = 4$ with just approximately 10° of inclination loss.

Table 2. Outgoing inclination (in deg) for different incoming and outgoing orbital periods between lunar encounters. Incoming inclination is 67° (aligned with polar axis).

Incoming \bar{P}	Outgoing \bar{P}			
	$1.5P_M$	$2.5P_M$	$3.5P_M$	$4.5P_M$
$1.5P_M$	67	61.56	58.45	56.40
$2.5P_M$	72.23	67	64.04	62.11
$3.5P_M$	75.03	69.89*	67	65.11
$4.5P_M$	76.81	71.71	68.86	67

These results open the way for different strategies for monitoring the North Pole and the South Pole alternatively. In fact, at the lunar swing-by, it is possible to decide the period of the next orbit, and therefore the time spent covering one pole, before switching to the other one.

The natural choice of the north and south orbits would be $\bar{P} = 6.5P_M$. This corresponds approximately to half a year, and with the proper synchronisation with the Sun, it would be possible to cover both the North Pole and the South Pole when illuminated by the Sun, in a similar fashion to what proposed by Heiligers et al. [16] Observing the pole when lit is particularly important, as it enables the acquisition of imagery in the visible band of the spectrum, which in turn provides essential data for meteorology and glaciology [3]. Unfortunately, the choice of $\bar{P} = 6.5P_M$ is not advisable, for two reasons: the first is that, for this orbit, no feasible swing-by exists to rotate the line of apsides; the second is that, due to its semi-major axis length, the orbit goes far away from the Earth, and the two-body approximation would start to become incorrect.

Fig. 6 and Fig. 7 and show one combination of north-south orbits, which is the one with an asterisk in Table 2 (in inertial and synodic frames respectively). The figure shows the trajectory in an inertial frame and in an Earth-Moon synodic frame. The translucent conical surface in Fig. 7 is the one described by the apparent rotation of the polar axis (which is inertially fixed) in the synodic reference. Both plots allow appreciate the difference in semi/major axis (and thus period) between the north and the south orbit, despite the inclination is very similar.

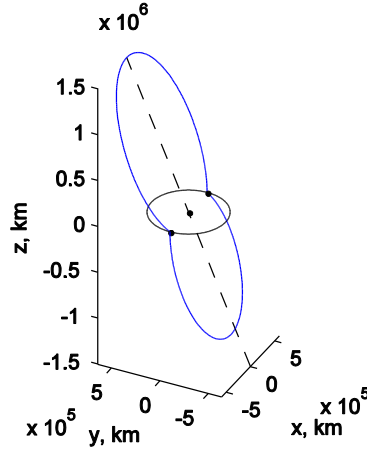


Fig. 6. Plot of trajectory (in Earth-centred inertial frame) with north orbit at 67° , $\bar{P} = 3.5P_M$, and south orbit at to 69.89° , $\bar{P} = 2.5P_M$. The lunar swing-by provides the manoeuvre to change the orbital elements.

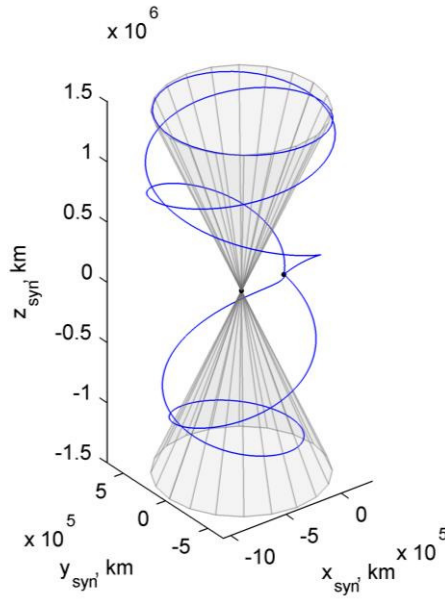


Fig. 7. Same as Fig. 6, in Earth-Moon synodic frame.

3.1. Continuous coverage analysis

With the aim of showing the coverage offered by the orbits, and in particular to show the continuous coverage of the polar regions, we consider the same figure of merit introduced in Ceriotti et al. [3] Referring to the geometry in Fig. 8, we define a minimum elevation angle of the spacecraft, ε_{\min} . The spacecraft, at latitude φ , is in sight of a point on the Earth's surface only if its elevation angle is $\varepsilon \geq \varepsilon_{\min}$. This angle defines a circular area centred in the sub-satellite point, such that any observer in this area is in sight of the spacecraft, at a given instant of time (yellow shaded area in Fig. 8). However, assuming that the motion of the spacecraft is much slower than the Earth's rotation around its axis, then it might happen that, due to the Earth's rotation, some points that at some time during the day are accessible, become inaccessible at some other time. Therefore the green area in Fig. 8 is defined by the latitude Λ above which any point on the Earth is in sight of the spacecraft, at any time of the day (i.e. for any angular position

of the Earth). The lower the value of Λ , the wider the area that is continuously covered (hence not just the polar caps, but also lower-latitude regions).

Clearly, one spacecraft is not sufficient to guarantee continuous coverage of one pole, despite that it can hover above it for a considerable amount of time. It was proposed to consider a constellation of three spacecraft (phased 120°) for the coverage of both poles [10].

Considering again the sample mission defined before (shown in Fig. 7 and marked with an asterisk in Table 2), Fig. 9 shows the latitude of the spacecraft φ and the minimum latitude of continuous coverage, Λ . It can be seen that, for the North Pole, combining the three spacecraft, the value of Λ does not go above 55° of latitude: this means that, above 55°N , any point on the Earth at any time of the day has at least one spacecraft in sight. The worst-case scenario for continuous coverage happens at the switching point between one spacecraft and the next one. In between, continuous coverage is available for latitudes well lower than 55° .

Moreover, it is important to underline that, for the orbit selected and for the North Pole, the switch between spacecraft happens every 55 days. This is a considerable amount of time, in which the same spacecraft can provide continuous coverage, as opposed to high-elliptical orbits around the Earth, in which the orbital period is about 12 hours. It was highlighted in the literature [4] the importance of an extended time window for monitoring the Earth's poles: it allows imaging at different times from the same point of view, and this allows the creation of the so-called atmospheric motion vectors, that are essential for weather forecasting. It is more complicated, and less precise, to compare images that are taken from different points of view, hence the necessity of a static (or almost static) platform.

In addition, the Moon provides the necessary Δv for flipping the apsides, and therefore similar coverage is available for the South Pole. If the same orbits were chosen for the north and the south, then the same coverage figures of merit would have been found.

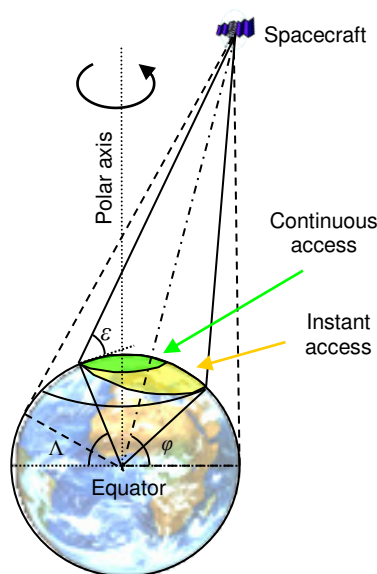


Fig. 8. Geometry of the spacecraft coverage.

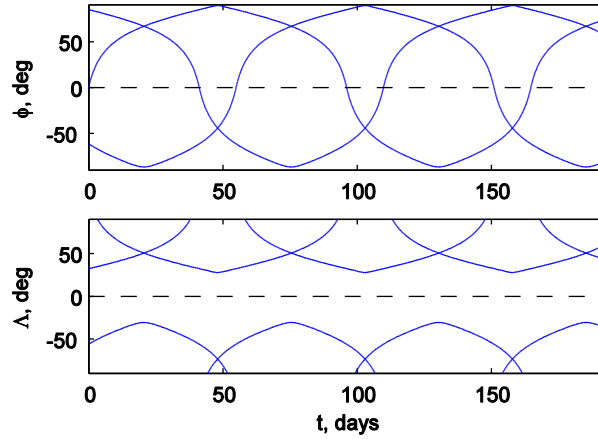


Fig. 9. Coverage figures for three spacecraft on trajectory represented in Fig. 7. (a) Latitude ϕ ; (b) Angle Λ . Both functions of time during the mission.

4. TRANSFER TO POLE-SITTER ORBIT

Breakwell et al. [17] presented a low-thrust transfer to a pole-sitter (in that work, named “pole-squatter”), which basically consisted in a transfer to a highly inclined, highly eccentric Earth orbit. The same idea is used in this work, where a preliminary approximation of the transfer to the pole-sitter position can be done by considering a highly eccentric orbit, the apocentre of which coincides with the pole-sitter position. However, we will also consider a breaking manoeuvre at the apocentre. This is due to the fact that this manoeuvre can have a non-negligible effect on the overall Δv of the transfer. Consequently, the inclination of this orbit over the Earth’s equator shall be 90° . In previous studies, this inclination was achieved either through a set of impulsive manoeuvres performed by the launcher main stage and/or upper stage [18], or (partly) by the low-thrust propulsion system of the spacecraft [17, 18]. However, it is well known that launcher performances are higher when the target orbit is equatorial (assuming the availability of an equatorial launch site). Therefore, it is worth investigating whether a gravity assist at the Moon can provide the necessary inclination change, in a way that the total cost of the transfer is less, and therefore more mass can be injected into the pole-sitter orbit, for the same mass injected into a LEO parking orbit by the launcher.

4.1. Transfer design

We consider a transfer strategy that relies on a single gravity assist of the Moon. Referring to Fig. 10, we assume a launcher with the capability of injecting a spacecraft and an upper stage into a circular equatorial LEO around the Earth. The upper stage then provides an impulsive manoeuvre Δv_{LEO} that transfers the spacecraft into a coplanar orbit (named incoming orbit) that encounters the Moon. Parameters of this orbit will be denoted with a superscript (-) because they refer to the orbit before the swing-by manoeuvre. The manoeuvre is:

$$\Delta v_{LEO} = \sqrt{\frac{2\mu}{r_{LEO}} - \frac{\mu}{r_{LEO}/(1-e^-)}} - \sqrt{\frac{\mu}{r_{LEO}}}$$

where $r_{LEO} = 200$ km is set arbitrarily and the eccentricity of the incoming orbit e^- is to be determined. Note that the minimum eccentricity to reach the Moon is:

$$e_{\min}^- = \frac{r_M - r_{LEO}}{r_M + r_{LEO}} \cong 0.9664$$

when the Moon is at the apocentre of the incoming orbit.

At the Moon, the swing-by is resolved using the method in Section 2.1. Figure 11 shows contour lines of constant outgoing inclination, function of the incoming orbit eccentricity and outgoing orbit apocentre. The graph is limited in the upper-left region by the feasibility condition of the swing-by (Eq. (8)).

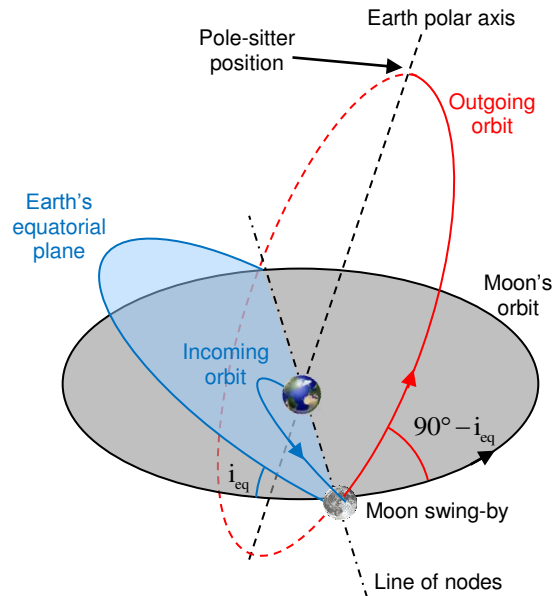


Fig. 10. Illustration of the transfer to the pole-sitter.

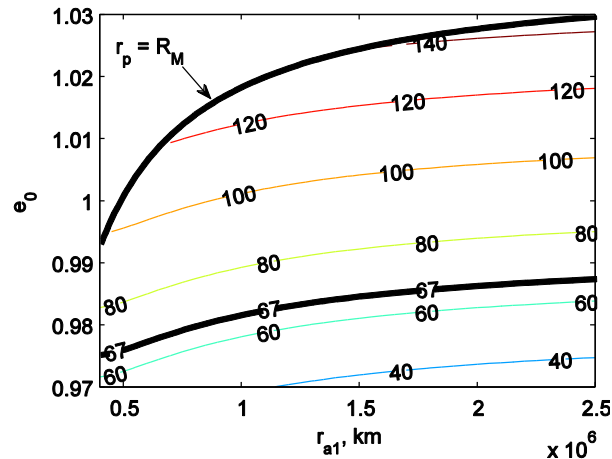


Fig. 11. Contours of constant inclination of outgoing orbit (in deg), function of incoming eccentricity and outgoing apocentre radius.

For the transfer under consideration, the inclination of the outgoing orbit is known: $i^+ = 90^\circ - i_{eq} = 67^\circ$, such that the apocentre is on the polar axis of the Earth. In addition, since we are interested in a North-Pole transfer, the argument

of pericentre is 270° , and $\gamma^+ > 0$. The spacecraft orbit after the swing-by, or outgoing orbit, is therefore determined in terms of a^+ , e^+ (function of e^-). This corresponds to the bold contour line in Fig. 11.

The apocentre of the outgoing orbit, r_a^+ , is chosen to match the pole-sitter position. However, it is necessary to consider a final braking manoeuvre Δv_a at the apocentre r_a^+ :

$$\Delta v_a = \sqrt{\frac{2\mu}{r_a^+} - \frac{\mu}{a^+}}$$

Due to the geometry of the orbits considered, and in particular the eccentricity being less than unity, the magnitude of this manoeuvre can be sensible. Conversely, in other types of transfers not involving the lunar swing-by [17], the eccentricity reaches values of approximately 1, and therefore this manoeuvre is negligible.

Note that, following this manoeuvre, a constant thrust is necessary to maintain the position, as discussed in previous work [19]. However, this is not part of the transfer, and therefore it will not be discussed here.

The total Δv for the transfer from LEO is therefore:

$$\Delta v = \Delta v_{LEO} + \Delta v_a \quad (9)$$

Fig. 12 shows contour lines for the total Δv , parameterised as in the previous Fig. 11. The black transversal contour line represents solutions in which $i^+ = 67^\circ$.

Fig. 13 shows the total Δv , as well as the two contributions as in Eq. (9), for the specific case under consideration of $i^+ = 67^\circ$. This figure can be imagined as a section of Fig. 11 along the contour line. Note that the manoeuvre at LEO increases very slowly with the apocentre of the target orbit, instead the magnitude of the manoeuvre at the apoapsis decreases rapidly. This makes it more economical to reach a steady pole-sitter position that is farther from the Earth, within the considered range of apocentre distances.

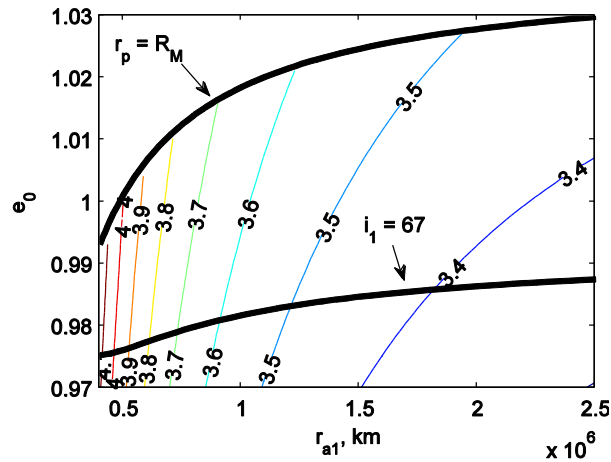


Fig. 12. Total Δv (as from Eq. (9)) function of function of incoming eccentricity and outgoing apocentre radius.

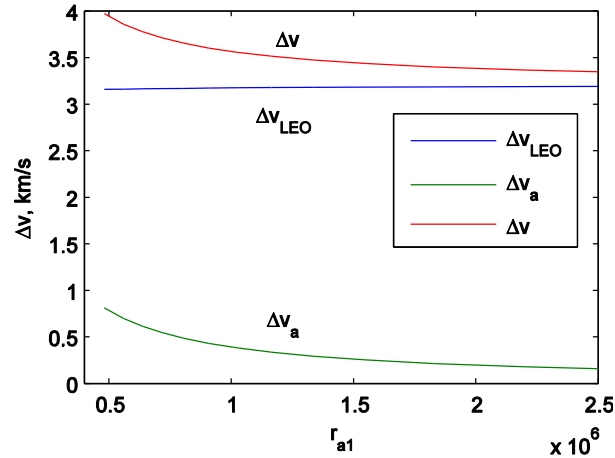


Fig. 13. Total Δv for reaching a stationary pole-sitter position, starting from a 200 km altitude circular equatorial orbit at the Earth.

We consider two pole-sitter mission profiles, corresponding to two different altitudes of the spacecraft. The first one, injects the satellite to 0.01 AU, that is 1.496×10^6 km, the second to 2.5×10^6 km. These two values are taken from the description of the poles-sitter mission [19], and the first is the distance of a constant-altitude reference mission, while the second is the average distance of a minimum-propellant hybrid or SEP pole-sitter mission.

By fixing the apogee r_a^+ , the incoming eccentricity e^- can also be found, and the transfer is fully determined. Plots of the orbits used in the transfer are in Fig. 14 for the two different distances. Note that although the full orbit is plotted, the spacecraft would only follow part of it during the transfer. Table 3 summarises the results for the two transfers.

Note that we assumed that the LEO is equatorial, and so is the incoming orbit. However, no launcher option of those considered here are equatorial, but their inclination is up to about 8° over the equator. It can be shown that small inclination changes do not change the results considerably. An inclination change in the incoming orbit corresponds to a rotation of the incoming velocity vector \mathbf{v}^- around the radial direction. Since the transversal and out-of-plane components of the vector are small compared to the radial one, it results that a change in inclination does not affect the lunar swing-by considerably, and consequently the total Δv of the transfer.

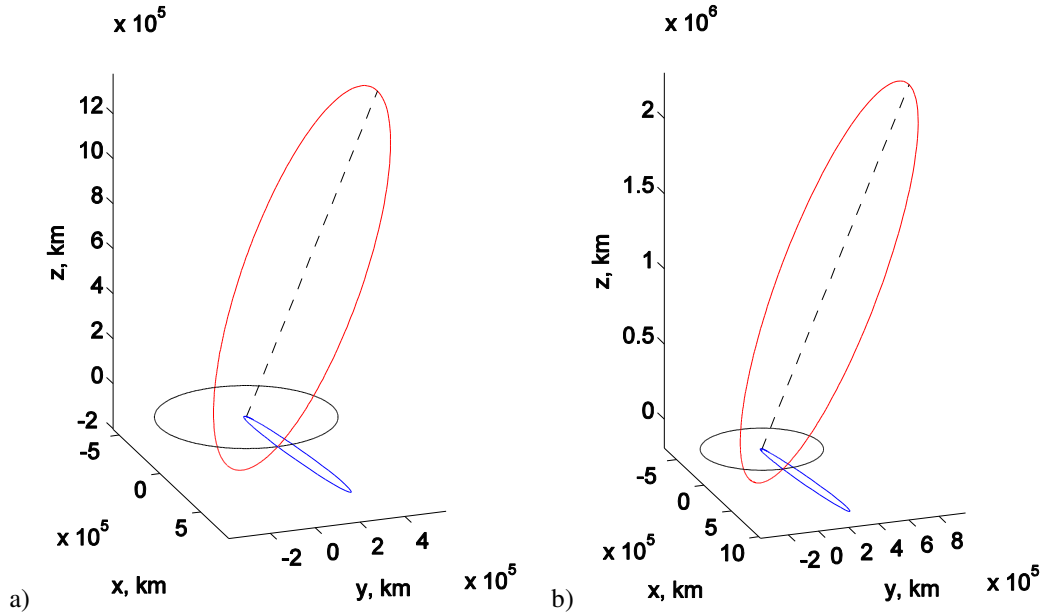


Fig. 14. The two orbits used in the transfer, patched by the lunar swing-by: incoming (blue) and outgoing (red) orbits. The dashed black line shows the polar axis of the Earth. (a) $r_a^+ = 1.496 \times 10^6$ km ; (b) $r_a^+ = 2.5 \times 10^6$ km .

Table 3. Details of transfers from LEO to two different distances of the pole-sitter.

Distance r_a^+ , km	Swing-by pericentre $r_{p, sb}$, km	Total Δv , km/s
1.496×10^6 km	4040 km	3.4441 km/s
2.5×10^6 km	4020 km	3.3467 km/s

4.2. Launcher performance

Given the trajectory and total velocity change required to transfer from LEO to the pole-sitter, in this section we provide an estimation of the mass that can be injected into the pole-sitter, considering two launcher options: Ariane 5 ECA and Soyuz CSG (launching from Kourou, French Guyana). The same launchers were considered in previous work, although the launch strategy was based on a sequence of impulses and/or low-thrust arcs in order to achieve the pole-sitter position, instead of a lunar swing-by. This will allow to compare the mass injected into pole-sitter orbit with that work, as a reference.

For both launchers, the manuals do not provide information for injection in the exact orbit computed in the previous section, therefore we will estimate the required data assuming impulsive manoeuvres of the upper stage, that join a circular LEO around the Earth to the target orbit.

In particular, the manual provides the total injected mass m^* into a given orbit a^*, e^* . We now assume that the injection into this orbit is performed from a circular LEO orbit, and therefore the impulsive velocity change can be computed as:

$$\Delta V^* = \sqrt{\frac{\mu}{r_{LEO}}} - \sqrt{\frac{2\mu}{r_{LEO}} - \frac{\mu}{a^*}}$$

This velocity change is provided by the upper stage of the launcher platform. The total mass that can be injected into LEO by the launcher (which includes propellant, upper stage, adapter and payload):

$$m_{LEO} = (m^* + m_{us}) e^{\frac{\Delta v^*}{g_0 I_{sp}}}$$

where m_{us} is the mass of the upper stage and its adapter, and I_{sp} its specific impulse, as provided in Table 4.

Since the total Δv for the transfer to the pole-sitter is known, and assuming again that the upper stage is providing the entire velocity change, then we can compute the injected mass into the pole-sitter position:

$$m_{ps} = m_{LEO} e^{-\frac{\Delta v}{g_0 I_{sp}}} - m_{us}$$

Table 4. Upper stage characteristics.

Launcher	Sp. impulse I_{sp} , s	Mass m_{us} , kg
Soyuz	330	1100
Ariane 5	446	4700

4.2.1. Soyuz CSG

For computing the deliverable mass by the Soyuz, we refer to the manual [20] where the performance (kg) is shown as a function of the altitude of the perigee of the target orbit. The perigee is at 250 km, and the inclination to 6° . Since the inclination is low, and as noted before does not affect considerably the Δv , inclination changes are neglected here. The plot, taken from the manual, is reproduced in Fig. 15. It can be seen that the graph does not include altitude of apocentre above 80,000 km. Therefore, we take the GTO reference, where we have:

$$a^* = 2.4753 \times 10^4 \text{ km}$$

$$e^* = 0.7322$$

Applying the previous formulas it is found that Soyuz can inject 2101 kg at 0.01 AU and 2199 kg at 2.5×10^6 km.

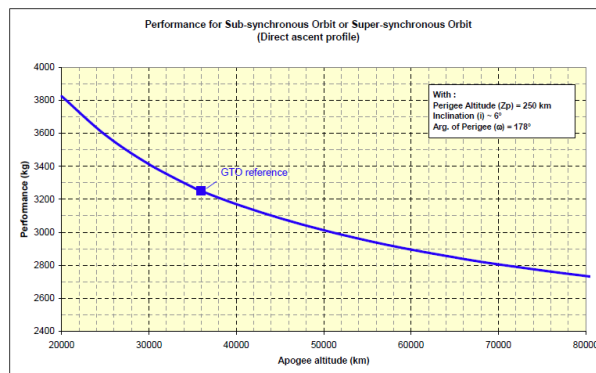


Fig. 15. Performance of Soyuz (kg of payload) for elliptic orbits (function of apogee altitude) with low inclination. [Figure from Soyuz User’s Manual [20]]

4.2.2. Ariane 5

The Ariane 5 manual does not provide a plot similar to that in Fig. 15 for Soyuz. Instead, some reference target orbits are listed as typical mission profiles [21]. The most similar profile is the “injection towards the Moon”, for which

7000 kg can be inserted into an orbit with apogee and perigee altitude of 385,600 km and 300 km respectively. This corresponds to:

$$a^* = 1.9933 \times 10^5 \text{ km}$$

$$e^* = 0.9665$$

The orbit is also inclined 12° , but again this does not affect the arrival velocity at the Moon considerably. In fact, an equatorial launch could possibly improve the performance of the launcher.

Using these values, it results that 6135 kg and 6379 kg can be injected in the near and far pole-sitter positions, respectively.

4.2.3. Summary

Table 5 shows a summary of the results in terms of mass that can be injected into two different pole-sitter positions. As a reference, it was found in previous work [18] that, by using the same launchers in combination with solar electric propulsion, the mass that can be injected into pole-sitter is about 1450 kg with Soyuz and 4450 kg with Ariane 5, with very small variations for different altitude of the injection point.

It shall be underlined that, although these results provide an indication of the mass that can be injected into the pole-sitter orbit, they cannot be directly compared to what is found in Heiligers et al. [18], because in that work, in the last part of the transfer the effect of the gravitational attraction of the Sun was taken into account. On the other hand, if SEP were employed for these types of transfer, it could be that the Δv for braking at the apogee would be distributed in a low-thrust arc that starts just after the lunar swing-by. The gravity losses of a distributed thrust arc would presumably increase the necessary Δv , but the higher specific impulse of the solar electric propulsion (of the order of 3000 s, one order of magnitude bigger than what offered by the upper stages) could indeed compensate, possibly allowing overall propellant saving.

In addition, the lunar swing-by increases considerably the complexity of the transfer, in terms of spacecraft operations, mainly due to the accuracy that is necessary for targeting the Moon, and due to the intrinsic risk of the swing-by manoeuvre (missing the correct hyperbola would almost certainly bring the spacecraft on a non-recoverable path).

All these issues shall be taken in a trade-off with the additional spacecraft mass that the lunar swing-by makes potentially available.

Table 5. Mass injected into pole-sitter position, m_{ps} , kg.

Distance, r_a^+	Ariane 5	Soyuz
1.496×10^6 km	6135	2101
2.5×10^6 km	6379	2199

5. CONCLUSION

This work has shown the capabilities offered by the lunar swing-by manoeuvre for generating trajectories for polar Earth observation, resonant with the Moon. It was shown that the Moon can be used to flip the line of apsides of an eccentric, highly-inclined orbit, enabling the possibility to switch between north and south coverage at no cost. With

small changes in inclination, it is also possible to modify the resonances with the Moon, therefore changing the time spent on each pole.

The swing-by of the Moon was also used to generate transfers to the pole-sitter orbit, and it was shown that, at the cost of additional complexity due to the swing-by, more mass could be injected into pole-sitter position.

Third body effects were not considered in this work, however some of the proposed orbits reach significant distances from the Earth, and therefore it is expected that the perturbation of the Sun would become important. Additional, future studies are necessary to quantify the corrections necessary to keep the spacecraft on-track, both in the case of elliptic orbits for Earth observation, and transfers to pole-sitter.

ACKNOWLEDGEMENTS

This work was conceived as part of European Research Council project 227571 VISIONSPACE, at the University of Strathclyde.

REFERENCES

- [1] P.C. Anderson, M. Macdonald, Extension of the Molniya orbit using low-thrust propulsion, 21st AAS/AIAA Space Flight Mechanics Meeting, AIAA, New Orleans, USA, 2011.
- [2] J.R. Wertz, W.J. Larson, Space mission analysis and design, third edition, Space technology library, Microcosm press/Kluwer Academic Publishers, El Segundo, California, USA, 1999.
- [3] M. Ceriotti, B.L. Diedrich, C.R. McInnes, Novel mission concepts for polar coverage: an overview of recent developments and possible future applications, *Acta Astronaut*, 80 (2012) 89-104. DOI: 10.1016/j.actaastro.2012.04.043.
- [4] M.A. Lazzara, A. Coletti, B.L. Diedrich, The possibilities of polar meteorology, environmental remote sensing, communications and space weather applications from Artificial Lagrange Orbit, *Adv Space Res*, 48 (2011) 1880-1889. DOI: 10.1016/j.asr.2011.04.026.
- [5] C.R. McInnes, P. Mulligan, Final report: telecommunications and Earth observations applications for polar stationary solar sails, National Oceanographic and Atmospheric Administration (NOAA)/University of Glasgow, Department of Aerospace Engineering, 2003.
- [6] J.M. Driver, Analysis of an arctic polesitter, *J Spacecraft Rockets*, 17 (1980) 263-269. DOI: 10.2514/3.57736.
- [7] M. Ceriotti, J. Heiligers, C.R. McInnes, Novel pole-sitter mission concepts for continuous polar remote sensing, *SPIE Remote Sensing*, Edinburgh, United Kingdom, 2012. DOI: 10.1117/12.974604.
- [8] T.J. Waters, C.R. McInnes, Periodic orbits above the ecliptic in the solar-sail restricted three-body problem, *J Guid Control Dynam*, 30 (2007) 687-693. DOI: 10.2514/1.26232.
- [9] R.L. Forward, Statite: a spacecraft that does not orbit, *J Spacecraft Rockets*, 28 (1991) 606-611. DOI: 10.2514/3.26287.
- [10] M. Ceriotti, C.R. McInnes, Natural and sail-displaced doubly-symmetric Lagrange point orbits for polar coverage, *Celest Mech Dyn Astr*, 114 (2012) 151-180. DOI: 10.1007/s10569-012-9422-2.
- [11] C. Uphoff, M.A. Crouch, Lunar cycler orbits with alternating semi-monthly transfer windows, *Advances in the Astronautical Sciences*, 75 (1991) 163-170.

- [12] P. Pergola, Low-thrust transfer to backflip orbits, *Adv Space Res*, 46 (2010) 1280-1291. DOI: 10.1016/j.asr.2010.06.018.
- [13] D.J. Dichmann, E.J. Doedel, R.C. Paffenroth, The computation of periodic solutions of the 3-body problem using the numerical continuation software AUTO, *International Conference on Libration Point Orbits and Applications*, Aiguablava, Spain, 2002.
- [14] M.H. Kaplan, *Modern spacecraft dynamics and control*, John Wiley and Sons, Inc., New York, 1976.
- [15] C. Uphoff, *The art and science of Lunar gravity assist*, AAS/GSFC International Symposium on orbital Mechanics and Mission Design, NASA-GSFC, USA, 1989.
- [16] J. Heiligers, M. Ceriotti, C.R. McInnes, J.D. Biggs, Design of optimal transfers between North and South pole-sitter orbits, 22nd AAS/AIAA Space Flight Mechanics Meeting, Univelt, inc., Charleston, South Carolina, USA, 2012.
- [17] J.V. Breakwell, O.M. Golan, Low thrust power-limited transfer for a pole squatter, *AIAA/AAS Astrodynamics Conference*, AIAA, Minneapolis, MN, USA, 1988, pp. 717-722.
- [18] J. Heiligers, M. Ceriotti, C.R. McInnes, J.D. Biggs, Design of optimal Earth pole-sitter transfers using low-thrust propulsion, *Acta Astronaut*, 79 (2012) 253–268. DOI: 10.1016/j.actaastro.2012.04.025.
- [19] M. Ceriotti, C.R. McInnes, Generation of optimal trajectories for Earth hybrid pole-sitters, *J Guid Control Dynam*, 34 (2011) 847-859. DOI: 10.2514/1.50935.
- [20] Arianespace, *Soyuz User's Manual - Issue 2 Revision 0*, Arianespace, 2012.
- [21] Arianespace, *Ariane 5 User's Manual - Issue 5 Revision 1*, Arianespace, 2011.

Vitae

MATTEO CERIOTTI



Dr. Matteo Ceriotti received his M.Sc. summa cum laude from Politecnico di Milano (Italy) in 2006 with a thesis on planning and scheduling for planetary exploration. In 2010, he received his Ph.D. on “Global Optimisation of Multiple Gravity Assist Trajectories” from the Department of Aerospace Engineering of the University of Glasgow (United Kingdom). During 2009-2012, Matteo was a research fellow at the Advanced Space Concepts Laboratory, University of Strathclyde, Glasgow, leading the research theme “Orbital Dynamics of Large Gossamer Spacecraft”. In 2012, he returned to the University of Glasgow as a lecturer in Space Systems Engineering, within the School of Engineering. His main research interests are space mission analysis and trajectory design, orbital dynamics, trajectory optimisation, particularly focusing on high area-to-mass ratio structures.

COLIN MCINNES



Colin McInnes is Director of the Advanced Space Concepts Laboratory at the University of Strathclyde. His work spans highly non-Keplerian orbits, orbital dynamics and mission applications for solar sails, spacecraft control using artificial potential field methods and is reported in over 150 journal papers. Recent work is exploring new approaches to spacecraft orbital dynamics at extremes of spacecraft length-scale to underpin future space-derived products and services. McInnes has been the recipient of awards including the Royal Aeronautical Society Pardoe Space Award (2000), the Ackroyd Stuart Propulsion Prize (2003) and a Leonov medal by the International Association of Space Explorers (2007).